INSTITUT DE FRANCE
Académie des sciences

Comptes Rendus

Chimie

Özlen Altun and Melike Özge Koçer

Pt(II) complex of Schiff base derived from L-phenylalanine and furfuraldehyde in the presence of 8-hydroxyquinoline: Structural analysis, composition of complex and biological activity

Volume 23, issue 2 (2020), p. 127-142

Published online: 19 June 2020

https://doi.org/10.5802/crchim.9

Les Comptes Rendus. Chimie *sont membres du*
Centre Mersenne pour l'édition scientifique ouverte
www.centre-mersenne.org
e-ISSN : 1878-1543

Comptes Rendus
Chimie
2020, 23, nº 2, p. 127-142
https://doi.org/10.5802/crchim.9

Full paper / *Mémoire*

Pt(II) complex of Schiff base derived from L-phenylalanine and furfuraldehyde in the presence of 8-hydroxyquinoline: Structural analysis, composition of complex and biological activity

Özlen Altun*, [a] and Melike Özge Koçer [a]

[a] Trakya University, Department of General and Inorganic Chemistry, 22030 Edirne/TURKEY.

E-mails: ozlenaltun@yahoo.com (Ö. Altun), ozge__kocer22@hotmail.com (M. O. Koçer).

Abstract. In the present study, we synthesized a Schiff base (L^1) derived from L-phenylalanine with furfuraldehyde and its Pt(II) complex ([Pt(L^1)(L^2)]: [Pt(N-(furfuralidene)phenylalanine)(8-hydroxyquinoline)]) in the presence of 8-hydroxyquinoline (L^2). The chemical structures of the synthesized Schiff base and Pt(II) complex were characterized using ESI-MS, UV–Visible, FT-IR, ^{1}H NMR, ^{13}C NMR, and powder-XRD spectroscopy. The surface morphologies and elemental composition were determined by SEM and EDX. Thermal analysis was performed with TG-DTA. Mole ratio of Meyer and Job methods were used for the composition of complexes. According to these methods, the ratio [Pt^{2+}] : [$L^1 + L^2$] was found to be 1 : 1. In addition, the antimicrobial activities of L^1 and the complex showed that the compounds have significant antibacterial and antifungal properties. They also show important cytotoxic effects against the growth of mouse embryo fibroblasts (MEF) and human prostate adenocarcinoma (Du145) cancer cells. L^1, L^2, and the Pt(II) complex also displayed effective antioxidant activity.

Keywords. Synthesis, Spectral Characterization, Antimicrobial Activity, Cytotoxic Activity, Antioxidant Activity.

Manuscript received 3rd October 2019, revised 19th November 2019, accepted 22nd November 2019.

* Corresponding author.

1. Introduction

Schiff bases are an important class of ligands that help to elucidate the mechanisms of various reactions in biological and chemical systems due to the presence of an imine group in their structures. Schiff bases have a significant role in coordination chemistry since they easily form stable complexes with most of the transition metal ions. Schiff bases containing nitrogen and oxygen donor atoms can be obtained by the condensation of various aldehydes and amines. Due to their structural and functional properties, Schiff bases derived from aldehydes and amino acids with transition metal ions have various applications in chemical, biological, and medical fields [1–5]. These compounds also have antimicrobial and antifungal activities against certain bacteria and fungal strains, respectively [6–9].

Metal complexes of Schiff bases derived from amino acids play a significant role in the investigation of DNA-binding and bovine serum albumin (BSA)-binding properties. DNA-binding metal complexes have been extensively investigated as potential anticancer drugs, DNA-dependent electron transfer, DNA structural and conformational probes [10]. Apart from DNA, many other proteins such as serum albumins, which are the most abundant proteins in the blood, are also extensively important in the accumulation and transportation of various drug molecules [11]. BSA is generally selected as a target protein due to its low cost and similarity to human serum albumin (HSA) [12]. Previously, DNA and BSA-binding properties of metal-based Schiff base complexes were investigated by Wei's [13–15] and Guo's groups [16–18]. For example, two hexacoordinated octahedral nickel (II) complexes [14] of Schiff bases derived from o-vanillin/salicylaldehyde with glutamine and an Ni(II) complex [15] of Schiff base of o-vanillin and l-methionine in the presence of 1,10-phenanthroline were synthesized and characterized. The DNA-binding properties of Ni(II) complexes and the interactions of the nickel (II) complexes with BSA were studied by using spectroscopic analysis. In another study, vanadium complexes of Schiff bases derived from *o*-vanillin/L-valine [17] and L-serine/2-hydroxy-1-naphthaldehyde in the presence of 1,10-phenanthroline [18] were synthesized and the binding properties studied. The results showed that the complexes can intercalate into calf thymus DNA (CT-DNA) and quench the intrinsic fluorescence of BSA in a static quenching process and cause conformational changes of BSA by binding to the BSA.

There are many methods which characterize Schiff bases derived from amino acids and aldehydes in the presence of various metals [19–23]. The Pt(II) complexes were found to act as active homogeneous catalysts in hydrogenation reactions [24], oxidative hydrolysis [25,26] of olefins, and activation of alkanes [27]. Since the platinum ions have the ability to form complexes, they bind to amino acids. Although there are many reports of transition metal complexes of Schiff bases derived from amino acids, information about the corresponding platinum(II) derivatives is still limited [28]. For these reasons, in this study, a Pt(II) complex [Pt(L^1)(L^2)] was synthesized using a Schiff base (L^1) derived from L-phenylalanine with furfuraldehyde in the presence of 8-hydroxyquinoline. The structure of the complex was investigated by Electrospray ionization mass spectrometry (ESI-MS), UV–Visible spectroscopy, Fourier transform infrared spectroscopy (FT-IR), ^{1}H nuclear magnetic resonance (NMR), ^{13}C NMR, powder-X-ray diffraction (XRD), scanning electron microscopy (SEM), energy-dispersive X-Ray analysis (EDX) and thermogravimetric and differential thermal analysis (TG-DTA). As a result of physicochemical, spectral, and thermal analyses, it was found that one molecule of L^1 and one molecule of L^2 react with one Pt^{2+} ion. The Schiff base and the complex were examined for antibacterial activities against *Escherichia coli* ATCC 25922, *Salmonella thyphimirium* ATCC 14028, *Listeria monocytogenes* ATCC19115, gram positive *Staphylococcus aureus* ATCC 25923, *Bacillus cereus* ATTCC 11778 and antifungal activity against *Candida albicans* ATCC 1023. These results are compared with the antibiotic ampicillin and the antifungal amphotericin B. The Schiff base and the Pt(II) complex were also investigated for cytotoxic activity against mouse embryo fibroblasts (MEF ATCC®SCRC-1008™) and human prostate adenocarcinoma (Du145 ATCC®HTB-81™) cells. In addition, antioxidant activities were determined for the obtained Schiff base and complex.

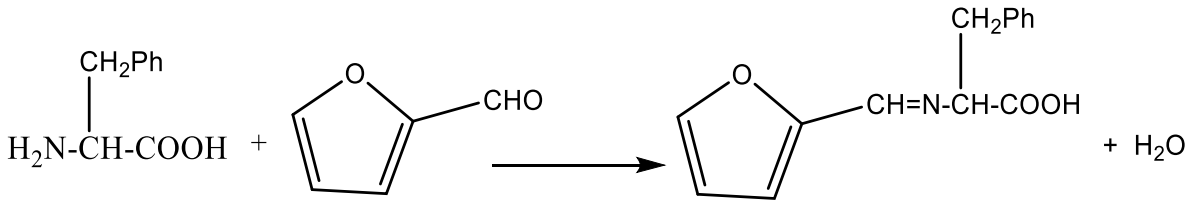

Scheme 1. The synthesis of Schiff base (L^1).

2. Experimental section

2.1. *Materials*

L-phenylalanine, furfuraldehyde, 8-hydroxyquinoline, methanol, *n*-heptane, and K_2PtCl_4 were purchased from Sigma, Aldrich, and Merck and used as supplied.

2.2. *Physical measurements*

Elemental analysis for C, H, N, and O were performed with a Costech ECS 4010 CHNSO element analyzer and an ICP-MS 7700X (Agilent) element analyzer was used for Pt. Conductivity measurements were done with an Inolab Thermal 740P in dimethylformamide (DMF). The magnetic moments were determined by an MK-1 Sherwood scientific magnetic susceptibility balance. ESI-MS was performed on an Agilent 6400 Series Triple Quadrupole. UV–Visible spectra were measured with a Shimadzu UV-1700 Pharma spectrophotometer in the wavelength range of 200–800 nm. FT-IR spectra were recorded in transmission mode by a Shimadzu FT-IR-470 spectrometer in the wavenumber range of 4000–400 cm^{-1}. KBr was used as matrix material for pellets. ^1H and ^{13}C NMR spectra were performed in D_2O for Schiff base and CD_3OD for the complex on a Bruker, DPX-400 spectrometer. A Shimadzu XRD-6000 was used for XRD analysis. SEM analysis was performed with a scanning electron microscope, model ZEIS LEVO LS 10. EDX was completed on an EVO LS 10 analyzer. The TG-DTA curves were recorded with a Seiko Exstar TG-DTA 6200 thermal analyzer with a heating rate of 10 °C·min^{-1} in the static atmosphere of dry air at a temperature range of 25–1200 °C. Platinum crucibles of 5–10 mg sample size were used in the analysis.

2.3. *Synthesis of Schiff base (L^1)*

The reaction mixture, including a methanolic solution (20 mL) of furfuraldehyde (1 mmol, 0.08 mL) and a solution of L-phenylalanine (1 mmol, 0.20 g) in methanol (20 mL) were refluxed for 3 h at 70 °C. Then the solvent was removed by evaporation. The obtained yellow crystals were recrystallized from water. The reaction is given in Scheme 1.

L^1 ($C_{14}H_{13}O_3N$): Yield (%): 88. Color: Yellow. M.P. (°C): 225. Elemental Analysis (%): Calcd.: C 69.13, H 5.35, O 19.75, N: 5.76; Found: C 69.08, H 5.30, O 19.69, N: 5.70. ESI-MS (*m/z*): Calcd. for L^1 $[M + H]^+$: 244. Found: 243.

2.4. *Synthesis of the Pt(II) complex in the presence of L^1 and L^2*

The L-phenylalanine (1 mmol, 0.16 g) was dissolved in 20 mL methanol containing NaOH (2 mmol, 0.08 g) and stirred magnetically at room temperature. Then, 0.08 mL furfuraldehyde (1 mmol), solid K_2PtCl_4 (1 mmol, 0.10 g), and 8-hydroxyquinoline (1 mmol, 0.14 g) in 10 mL methanol were added to the solution and the mixture was stirred magnetically for 3 hours at room temperature. The solution volume was reduced 75% by evaporation. The obtained brown solid was recrystallized from methanol.

[Pt(L^1)(L^2)]([Pt($C_{14}H_{12}O_3N$)(C_9H_6ON)]): Yield (%): 82. Color: Brown. M.P. (°C): 195. Elemental Analysis (%): Calcd.: C 47.49, H 3.09, O 11.01, N 4.82, Pt: 32.56; Found: C 47.44, H 3.06, O 10.98, N 4.79, Pt: 33.57. Magnetic Moment (μ_{eff}, BM): 0.00, Diamagnetic. Conductivity (Ω^{-1} cm^2 mol^{-1}): 27.5, ESI-MS (*m/z*): Calcd. for [[Pt(L^1)(L^2)] $[M + H]^+$: 582.09. Found: 581.08. Accordingly, the following reaction was determined:

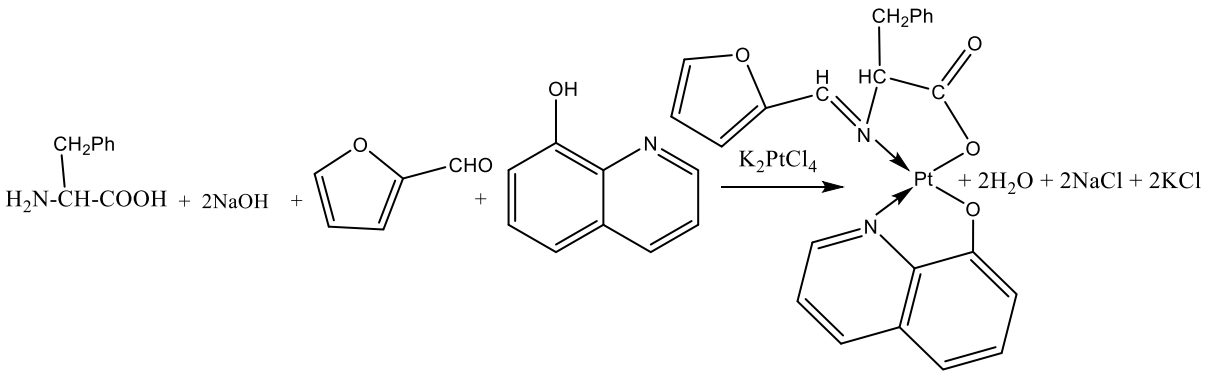

Scheme 2. The possible reaction of the Pt(II) complex with L^1 and L^2.

2.5. *Antimicrobial activity*

Since antimicrobial properties of L^2 were reported in previous studies [29–32], in this study, antimicrobial activities of the synthesized L^1 and Pt(II) complex were evaluated using the broth micro-dilution method and the Clinical and Laboratory Standards Institute (CLSI) procedures [33–38]. Minimal Inhibitory Concentration (MIC) values for each compound were determined against three gram-negative bacteria (*Escherichia coli* ATCC 25922, *Salmonella typhimurium* ATCC 14028, and *Listeria monocytogenes* ATCC19115); two gram-positive bacteria (*Staphylococcus aureus* ATCC 25923 and *Bacillus cereus* ATTCC 11778); and fungal (*Candida albicans* ATCC 1023) strains. The area of the zone of inhibition was measured using ampicillin and amphotericin B (positive control) for bacterial and fungal strains, respectively. The concentrations of tested compounds were prepared in the range 200–6.25 μg/mL. Dimethyl sulfoxide (DMSO), which has no activity, was used as negative control. Microorganisms were seeded in a 96-well sterile microplate. The microplate was then incubated for the growth of test organisms for 24 h at 37 °C. The absorbance was measured on a Thermo Multiscan GO Microplate Reader Spectrophotometer at 600 nm. The color change was determined visually. Any color change from purple to pink was considered as positive. The lowest concentration with a color change was recorded as the MIC value. All experiments were repeated four times.

2.6. *Cytotoxic activity*

Anticancer therapy is generally used with chemotherapeutic compounds that promote the destruction of sensitive tumors and show cytotoxic activity against cell proliferation [39,40]. The cell viability was evaluated with the MTT method [41–44]. The MTT assay is a well-documented cell viability assay for cytotoxic activity that was first tested by Mosmann [45]. The MTT assay can be applied to any cancer cell because MTT can be metabolized by all living cells. In this analysis, cells were cultured in Dulbecco's Modified Eagle Medium supplemented with 10% fetal bovine serum, 1% L-glutamine, 5% heat-inactivated penicillin–streptomycin (100 IU/mL) and kept in a 5% CO_2 incubator at 37 °C. Healthy human (MEF, ATCC®SCRC-1008™) cells and human prostate adenocarcinoma (Du145, ATCC®HTB-81™) cancer cells were transferred into a 96-well sterile microplate using a culture medium (density of approximately 7500 cells/well in 200 μL) for 24 h. The cell viability was determined with trypan blue dye using a hemocytometer and a 95% viability was confirmed. For cell attachment, the microplate was incubated in a 5% carbon dioxide incubator for 24 h at 37 °C. After 24 h, synthesized Pt(II) complex in the concentration of 25, 50,100, 200, 400, and 800 μM was added to the wells and again kept in incubation for 24 h. Then, 20 μL/200 μL per well of 5 mg/mL MTT (3-(4,5-dimethyl-thiazol-2-yl)-2,5-diphenyltetrazolium bromide) solution was added and incubated at 37 °C for an additional 4 h. The formazan blue formed in the cells was dissolved in

DMF (200 µL/well). The optical density (OD) was measured on a Thermo Multiscan GO Microplate Reader Spectrophotometer at 490 nm. The measured absorbance value for each concentration of the Pt(II) complex was compared to the DMF-treated control. The IC_{50} values were evaluated. All experiments were performed six times. Growth inhibition percentage was calculated with the following formula [46]:

$$\text{Growth inhibition \%} = \frac{\text{OD control} - \text{OD treated sample}}{\text{OD control}} \times 100 \quad (1)$$

2.7. *Antioxidant activity*

The stable DPPH (2,2-Diphenyl-1-picrylhydrazyl) radical scavenging assay is a widely used method to evaluate antioxidant activities, as it is a simple and rapid method compared to others [47–52]. Different concentrations of the free ligands and Pt(II) complex were dissolved by serial dilution in methanol to attain final concentrations ranging from 1 to 5 µg/mL. The prepared solutions were added to a sterile 96-well microplate. BHT (2,6-di-tert-butyl-4-methylphenol) was used at a concentration range of 1–5 µg/mL in methanol as positive control. Methanol was chosen for blanks. After 1 h of incubation in the dark, the absorbance (A) was recorded against a blank at 517 nm on a Tecan-PC infinite M200 Pro Plate reader and IC 50 (50% inhibition of DPPH color) values were calculated. Experiments were duplicated. DPPH inhibition percentage (Antioxidant Activity %) was calculated using the following formula:

$$\text{Antioxidant \%} = \frac{A_{\text{blank}} - A_{\text{sample}}}{A_{\text{blank}}} \times 100, \quad (2)$$

where A_{blank} is the absorbance of the blank and A_{sample} is the absorbance of sample.

3. Results and discussion

Elemental analysis for C, H, N, and O is in accordance with the proposed general formula of L^1 and the Pt(II) complex. In order to determine the molar conductivity, the complex was dissolved in DMF 10^{-3} M at 25 °C. The molar conductivity Λ of the complex was calculated using the following formula:

$$\Lambda m = \frac{K}{C}, \quad (3)$$

where K is the measured conductivity (specific conductance) and C is the molar concentration of the complex solution. The molar conductivity value for this complex was 27.5 $\Omega^{-1}\cdot cm^2\cdot mol^{-1}$. Therefore, this complex can be considered as a non-electrolyte [53,54]. The magnetic moment of the complex was determined to be μ_{eff} = 0.00 BM: the complex is diamagnetic, in a low-spin state and with square-planar geometry.

In the ESI-MS of L^1 (Figure 1), the peak at m/z = 244 (found: 243) corresponds to $[M + H]^+$ of L^1 and supports the suggested structure in Scheme 1. The ESI-MS spectrum of the complex (Figure 2) shows a molecular pattern with maximum intensity at m/z = 582.09 (found: 581.08) that is compatible with $[M + H]^+$ for the structure presented in Scheme 2. The spectrum also shows isotope peaks at *m/z* 338, 339, and 340 corresponding to the molecular cation, resulting from removal of L^1 molecule from the parent ion.

The UV–Visible spectra of L^1, L^2, and their Pt(II) complex (Figure 3) in $CHCl_3$ showed absorption bands between 200 nm and 800 nm. While the electronic spectrum of L^1 contains three bands, L^2 has two bands in the UV region. The first bands for L^1 at 249 nm and for L^2 at 225 nm are assigned to π–π* and n–π* (–C=N, –C=O) transitions. The second bands of L^1 and L^2 at 305 and 275 nm, respectively, and the third band of L^1 at 404 nm may be ascribed to the long pair electrons of nitrogen and oxygen atoms. These values are shifted to higher values in the UV–Visible spectrum of the complex. The complex shows three absorption bands at 252, 354, and 416 nm which are attributed to $^1A_{1g} \rightarrow {}^1E_g$, $^1A_{1g} \rightarrow {}^1B_{1g}$ and $^1A_{1g} \rightarrow {}^1A_{2g}$ transitions, respectively. As a result, the observed transitions are consistent with low-spin square-planar geometry [55–61].

The FT-IR spectra of free ligands and their Pt(II) complex are detailed in Table 1. In the FT-IR spectrum of the complex, the symmetric and asymmetric vibrations of the –COO group are not observed since the amino acid-derived Schiff bases are not in the form of their salts. But the characteristic bands at 1597 and 1454 cm^{-1} which may be caused by the symmetric ν(COO) and asymmetric ν(COO) stretching vibrations, respectively, of the coordinated carboxylate group [62–69]. This assignment is based on the fact that non-ionized and uncoordinated ν(COO) stretching band occurs usually around 1750–1700 cm^{-1}, while the ionized and coordinated ν(COO) stretching appears around

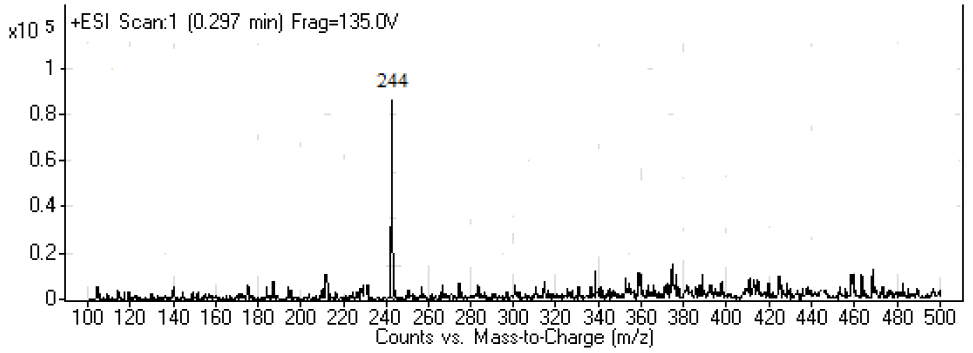

Figure 1. ESI-MS spectrum of L^1.

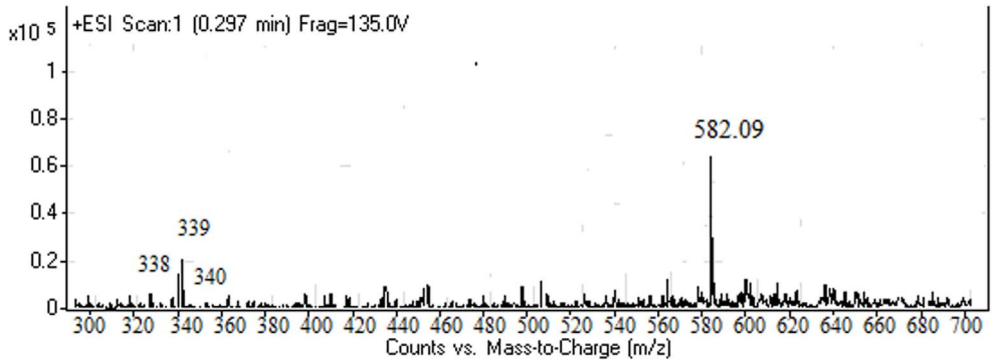

Figure 2. ESI-MS spectrum of the Pt(II) complex.

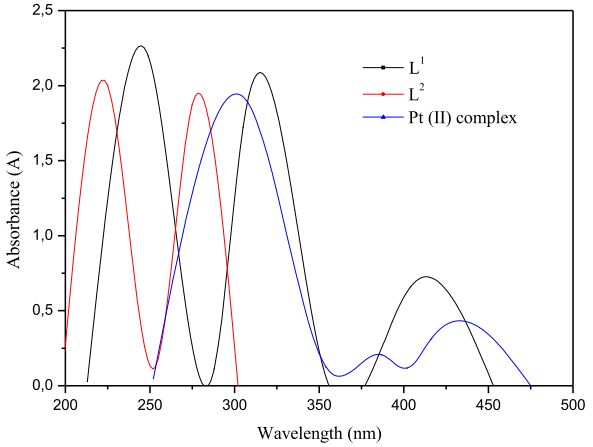

Figure 3. UV–Visible spectrum of L^1, L^2, and the Pt(II) complex.

1600–1400 cm^{-1}. In addition, in the FT-IR spectrum of L^1, the characteristic bands at 1635 and 1548 cm^{-1} are attributed to ν(C=N) and ν(C=C) stretching vibrations. These bands are shifted to 1643 and 1502 cm^{-1} in the complex, which indicates that the imino nitrogen and phenolic oxygen of the Schiff base are coordinated to the Pt(II) ion. The broad OH stretching band in the 3200–3100 cm^{-1} region for L^2 is missing in the spectrum of the complex. A significant feature of FT-IR spectra of the metal complexes in the presence of L^2 is the absence of band ~3440 cm^{-1} due to the OH stretching vibration of the free OH group in L^2. This observation leads to the conclusion that complex formation takes place by deprotonation of the hydroxyl group of the L^2 moiety. Furthermore, the stretching vibration of the azomethine, which appears at 1630 cm^{-1} in L^2, is shifted to a lower frequency in the complex, which indicates coordination through the ternary nitrogen donor of L^2 [63]. The coordination through the nitrogen atom in ν(C–N) and ν(C=N) groups is supported by the appearance of new bands at 598 cm^{-1} in the spec-

Table 1. Characteristic FT-IR bands (cm^{-1}) of the free ligands and Pt(II) complex

	L^1	L^2	Pt(II) complex
ν(OH)	-	3100	-
ν(COOH)	1709	-	-
ν(C=N)	1635	1630	1643
νas(COO)	-	-	1597
ν(C=C)	1548	1524	1502
νs(COO)	-	-	1454
ν(Pt–O)	-	-	698
ν(Pt–N)	-	-	598

trum of the complex which may be connected with the ν(Pt–N) vibration and a new band of weak intensity observed at 698 cm^{-1} which may be assigned to the ν(Pt–O) vibration [65].

^{1}H NMR (300 MHz, D_2O for Schiff base and CD_3OD for complex) (Table 2) and ^{13}C NMR (75 MHz, D_2O for Schiff base and CD_3OD for complex) (Table 3) spectra of free ligands and their Pt(II) complex were recorded to verify the binding of the Schiff base and 8-hydroxyquinoline molecules to the Pt^{2+} ion. For the Schiff base, the characteristic ^{1}H NMR signal at 9.2 ppm is assigned to the COOH proton. The peak at 7.7 ppm is attributed to the HC=N proton. The multiplets in the 6.5–7.4 ppm range are attributed to aromatic and furan protons. The two signals at 3.8 and 2.7 ppm are assigned to the aliphatic hydrogen protons (–CH and $–CH_2$, respectively) of the L-phenylalanine moiety. For the 8-hydroxyquinoline [70,71], the characteristic ^{1}H NMR signal at 9.7 ppm is attributed to the OH proton. The other six protons of the quinoline ring appear as multiplets between 6.7 ppm and 8.9 ppm. In the ^{1}H NMR spectrum of the complex, –OH and –COOH peaks are missing and little shifts are seen in the other peak positions. According to Table 4, the ^{13}C NMR spectrum of L^1 has signals at δ: 152 (s, C_1), 126 (s, C_2), 114 (s, C_3), 150 (s, C_4), 181 (s, C_5), 53 (s, C_6), 176 (s, C_7), 34 (s, C_8), 138 (s, C_9), 132 (s, C_{10} and s, C_{14}), 134 (s, C_{11} and s, C_{13}), and 130 ppm (s, C_{12}), whereas the ^{13}C NMR spectrum of L^2 shows signals at δ: 150 (s, C_1), 122 (s, C_2), 136 (s, C_3), 118 (s, C_4), 127 (s, C_5), 122 (s, C_6), 153 (s, C_7), 139 (s, C_8), and 127 ppm (s, C_9). ^{1}H and ^{13}C NMR data indicate that the complex was shifted in comparison with L^1 and L^2 [72].

Despite several attempts, [73,74], single crystal of the studied complex could not be obtained. Therefore, the XRD-powder pattern of the Pt(II) complex was investigated in order to test the degree of crystallinity of the complex [75–78]. The X-ray powder diffraction patterns of the complex were determined over 2θ = 5–80° and six important peaks were observed in the angle range of 10–70° (2θ), which arise from diffraction of X-rays by the planes of the complex (Figure 4). The inter-planar spacing (d) was found from the positions of intense peaks using Bragg's equation. Angle (2θ), inter-planar spacing (d), full-width at half-maximum (FWHM) of prominent intensity peak, intensity (%), and integrated intensity (%) are given in Table 4. According to Table 4, the 2θ values with maximum intensity of the peaks for the complex are determined to be 12.5206, 24.8819, 28.1212, 40.4385, 46.3102, and 66.7250 (2θ) which corresponds to d: 7.06402, 3.57558, 3.17064, 2.22879, 1.95895, and 1.40071 Å, respectively. There are good agreements between 2θ and d values. All the peaks calculated from the observed values of inter-planar distance were compared to the recorded one. The unit cell calculations were recorded for cubic symmetry from all significant peaks, and $h^2+k^2+l^2$ and (hkl) values were evaluated. The $h^2+k^2+l^2$ values are 1, 1, 1, 1, 2, 2.8 and the (hkl) values (000), (001), (001), (111), (200) and (220) for the Pt(II) complex. These results are compatible with characteristic XRD peaks of other Pt(II) complexes in the literature. The average crystallite size (D) of the complex dxrd was calculated using Scherrer's equation [79–82].

$$D = \frac{K\lambda}{\beta Cos\theta}, \tag{4}$$

where D is the particle size of the crystal, K is a constant, which is 0.94 for Cu grid, λ is the X-ray wavelength (1.5406 A), θ is the Bragg diffraction angle; and β is the FWHM. The complex has a crystallite size of 33 nm, suggesting that the complexes are in a nanocrystalline phase.

The surface of the Pt(II) complex was examined using SEM [83–85]. SEM is a simple method that indicates the structure of the surface of the prepared complex. SEM analyses the surface of the complex showing small to medium sized particles that tend to agglomerate in different ways compared to the starting materials. The SEM image of the complex

Table 2. ^{1}H NMR chemical shifts (δ/ppm) of the free ligands and Pt(II) complex

	L^1	L^2	Pt(II) complex
OH	-	9.7 (m,5H)	-
COOH	9.2 (s,1H)	-	-
HC=N	7.7 (s,1H)	-	7.5 (s,1H)
Ar.CH	6.5–7.4 (m,5H)	-	6.9–7.4 (m,5H)
Furan CH	6.5–7.4 (m,3H)	-	6.9–7.4 (m,3H)
8-Qring CH	-	6.7–8.9 (m,6H)	9.0–9.5 (m,6H)
CH	3.8 (t,1H)	-	4.9 (t,1H)
CH_2	2.7 (m,2H)	-	3.1–3.4 (m,2H)

Table 3. ^{13}C NMR chemical shifts (δ/ppm) of the free ligands and Pt(II) complex

	L^1	L^2	Pt(II) complex
C_1	152	150	160 and 152
C_2	126	122	130 and 125
C_3	114	136	117 and 140
C_4	150	118	153 and 121
C_5	181	127	185 and 128
C_6	53	122	56 and 115
C_7	176	153	180 and 158
C_8	34	139	38 and 145
C_9	138	127	142 and 131
C_{10}	132		136
C_{11}	134		138
C_{12}	130		133
C_{13}	134		138
C_{14}	132		136

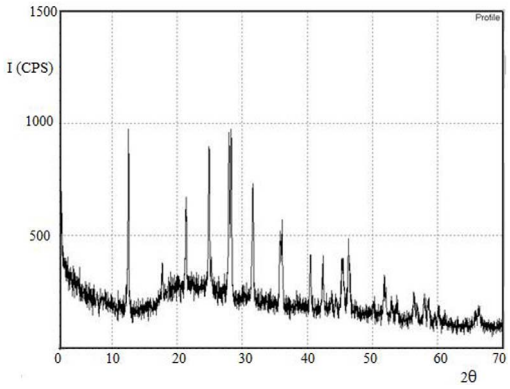

Figure 4. XRD patterns of the Pt(II) complex.

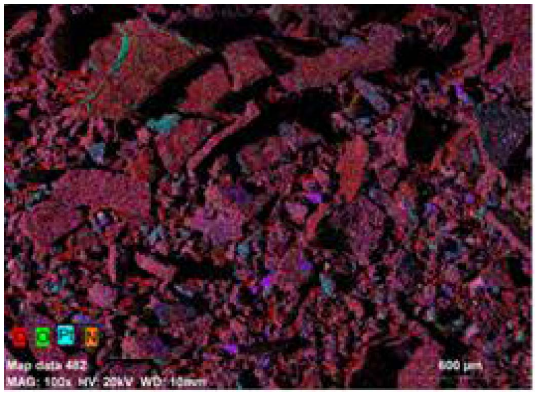

Figure 5. SEM image of the Pt(II) complex.

(Figure 5) shows that Pt(II) particles are spherical in size. The Pt(II) particles are quite visible throughout the complex as the presence of small grains in the nanometer range. In addition, EDX [83–85] was used for the elemental analysis on different sizes of nanoparticles from the complex (Figure 6). The results obtained by EDX indicated that there were platinum, carbon, oxygen, and nitrogen peaks and each metal ion for the formed Schiff base complex was distributed homogeneously.

TG-DTA values of the complex are given in Table 5. Three decomposition steps are obtained in the temperature range of 25–900 °C. The first decomposition in the range of 25–200 °C corresponds to the loss of 0.4%, which in turn corresponds to the loss of possible water molecules. The second decomposition in the range of 200–500 °C is the

Table 4. XRD analysis data of the Pt(II) complex

Strongest peak no	2θ (deg)	*d* (Å)	I/II	FWHM (deg)	Intensity (counts)	Integrated Intensity (counts)
9	12.5206	7.06402	88	0.25070	150	2138
22	24.8819	3.57558	84	0.25730	143	2045
27	28.1212	3.17064	100	0.56050	171	4491
38	40.4385	2.22879	38	0.23710	65	870
45	46.3102	1.95895	43	0.31550	74	1433
51	66.7250	1.40071	3	0.17000	14	166

Table 5. Thermal analysis data of the Pt(II) complex

Compound	Steps	Tb-Tc (°C)	Weight loss (%)	Assignments
Pt(II) complex	1st	25–200	0.4	Possible water molecule
	2nd	200–500	46.6	Organic Component
	3rd	500–900	53.4	PtO

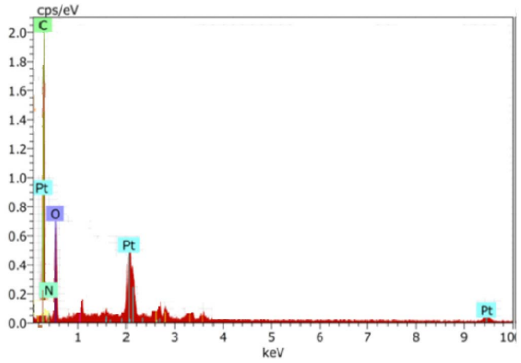

Figure 6. EDX analysis of the Pt(II) complex.

decomposition of the organic component (46.6%). The temperature range 500–1000 °C leads to the formation of platinum oxide (PtO, 53.4%) as a residue. These results indicate that the complex has good compatibility with the proposed structure. As a result of thermal analysis, qualitative conclusions can be made about the stability of the complex.

3.1. *Solution study*

The most commonly used method for determining the stability of a Pt(II) complex in a physiological medium is a time-based electronic spectrum study of the complex in a reference physiological buffer (50 mM phosphate, 4 mM NaCl, pH 7.4) [86–91]. The complex is poorly soluble in water, but its solubility is quite high in organic solvents such as $CHCl_3$, CH_3OH, and DMF. Therefore, the stability of the Pt(II) complex dissolved in a minimum amount of CH_3OH, followed by phosphate buffered saline (PBS), giving a final concentration of the complex 10^{-3} M at room temperature was evaluated using a UV–Visible spectrophotometer. In Figure 7, the observed transitions in the range of 300–450 nm, attributed to ligand to metal charge transfer bands, are stable over 18 hours. This result showed that the Pt(II) complex is stable when dissolved in a reference physiological buffer.

3.2. *Determination of the optimum conditions*

In order to evaluate the wavelength for the reactions, various solutions with pH values ranging from 1 to 10 of the molar composition ($L^1 + L^2$) with Pt(II) were arranged in the mole ratio of 1:1:1 ($L^1 + L^2 + Pt^{2+}$) and the spectra were obtained at room temperature. The complex produced an absorption band at λ = 416 nm. Since the absorbance became stable at pH values above 7 (Figure 8), the wavelength value λ = 416 nm and the pH value of 7 were chosen [92–94].

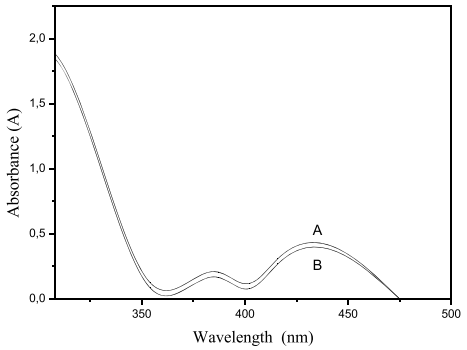

Figure 7. UV–Visible spectrum of the Pt(II) complex in physiological buffer at $t = 0$ (a) and $t = 18$ hours (b).

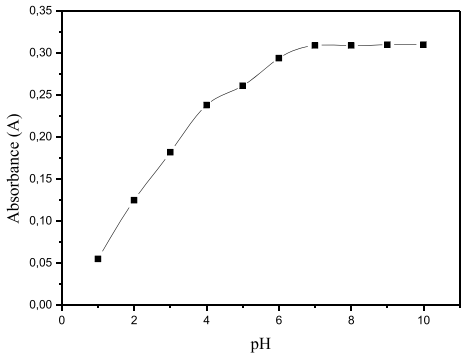

Figure 8. The effect of pH on absorbance.

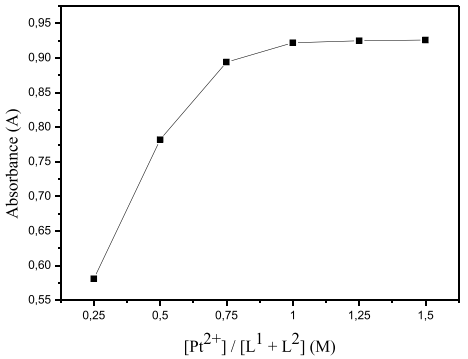

Figure 9. Determination of mole ratio.

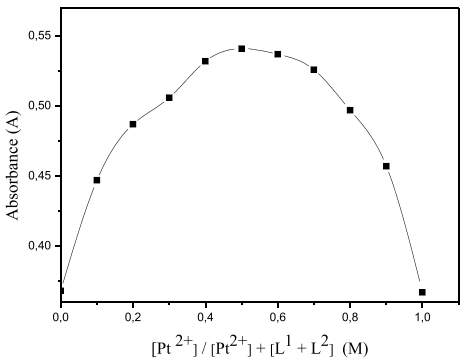

Figure 10. The composition of the Pt(II) complex.

3.3. *Composition of the Pt(II) complex*

The perpetual change method of mole ratio [95] and Job's method of continuous variations [96,97] were used for examination of the composition of the complex during the reaction. For the perpetual change method of mole ratio, various methanolic solutions were prepared at total concentrations of 2×10^{-3} M, under the general procedure, including $L^1 + L^2$ in the presence of Pt(II). The absorbances were recorded at 416 nm and the perpetual change graph (Figure 9) was plotted against $[Pt^{2+}]/[L^1 + L^2]$ after necessary absorbance adjustment. The perpetual change demonstrated one maximum for $[Pt^{2+}]/[L^1 + L^2] = 1$. For the Job's method, various solutions were prepared at total concentrations of 1×10^{-3} M under the general procedure, including $(L^1 + L^2)$ and Pt(II). The absorbances were recorded at 416 nm and the perpetual change graph (Figure 10) was plotted against $[Pt^{2+}]/([Pt^{2+}] + [L^1 + L^2])$. Job's method of continuous variations produced one maximum for the complex and is $[Pt^{2+}]/([Pt^{2+}] + [L^1 + L^2]) \sim 0.5$. According to Figures 9 and 10, one molecule of L^1 and one molecule of L^2 react with one Pt(II) ion.

3.4. *Antimicrobial activity results*

Antimicrobial properties of 8-hydroxyquinoline (L^2) were reported in previous studies, L^2 was determined to be a very strong antimicrobial agent against gram positive *S. aureus* and fungal *C. albicans* [29–32]. In this study, the antimicrobial activities of L^1 and the Pt(II) complex were evaluated by the micro-broth dilution method and MIC values were calculated. The antimicrobial activities of the L^1 and Pt(II) complex were examined against bacterial and fungal strains. The results are recorded in Figure 11 and Table 6. Previous studies about the antimicrobial activity of various Pt(II) complexes indicate a broad spectrum of

antibacterial and antifungal activity. Compared with antimicrobial activity data from previously reported literature [98–100], the Pt(II) complex have significant activity against *S. aureus, L. monocytogenes*, and *C. albicans* strains in our study. According to our antimicrobial activity results, while the obtained complex was effective against *S. aureus, L. monocytogenes*, and *C. albicans* at 6.25 µg/mL concentrations, L^1 showed moderate antibacterial activity against *S. aureus, L. monocytogenes*, and *C. albicans* at 12.5, 12.5, and 6.25 µg/mL concentrations, respectively. As a result of antimicrobial experiments, the synthesized complex shows increased activity compared with L^1 and L^2. The high activity of the Pt(II) complex may be due to the effect of Pt^{+2} ion on the normal cell membrane. The higher antibacterial activity of Pt(II) than L^1 and L^2 can be explained by chelation of L^1 and L^2 with Pt^{+2} since metal chelates display both polar and non-polar properties [101,102]. These properties make them suitable for permeation into cells. The polarity of the metal ion is reduced due to partial sharing of the positive charge of the metal ion with the donor groups, such as nitrogen and oxygen on L^1 and L^2. Chelation enhances the penetration of complex into lipid membranes by increasing the delocalization of π-electrons over the entire chelate ring [103,104]. It also increases the lipophilic nature of the central metal ions, leading to liposolubility through the lipid layer of cell membranes. The lipophilicity, which controls the rate of entry of molecules into the cell, is modified by coordination. Therefore, the obtained Pt(II) complex can become more active than the free L^1 and L^2 [105] and may be preferable to other inorganic complexes of platinum(II) due to its high effectiveness in preventing infection.

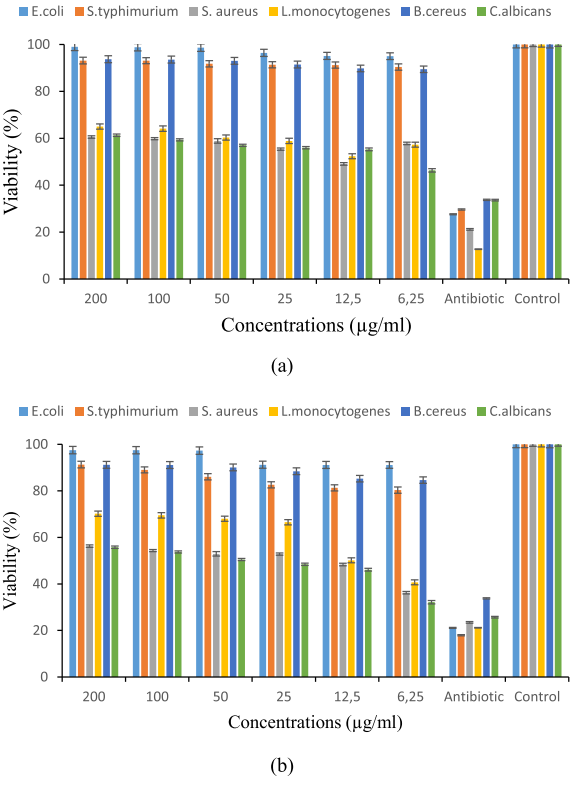

Figure 11. The viability (%) values for L^1 (a) and the Pt(II) complex (b) at different concentrations (200–6.25 µg/mL) for *E. coli*, *Salmonella thyphimirium*, *Staphylococcus aureus, Listeria monocytogenes, Bacillus cereus*, and *Candida albicans* ($n = 4$) ± S.E.

3.5. *Cytotoxicity results*

The coordination complexes of Pt(II) show interesting cytotoxic and antitumor properties [106–112]. Previously, many studies reported the cytotoxic properties of (L^2) 8-hydroxyquinoline [113,114]. Hence, in our study, the cytotoxic activities of L^1 and the Pt(II) complex were determined for MEF cells and Du145 cancer cells by an MTT assay. The results are presented in Figures 12 and 13. The IC_{50} values within the nanomolar range (50% inhibition) were evaluated from the dose response curves. The IC_{50} values of L^1 and Pt(II) complex for MEF were calculated as >1000 µM and >1000 µM. For the Du145, the IC_{50} values of L^1 and Pt(II) were determined as 77 µM and 41 µM, respectively. According to the analysis results, no death was observed in MEF cells at any concentration, whereas L^1 was effective on Du145 cancer cells at 100, 200, 400, and 800 µM concentrations. The complex showed significant effect on Du145 cancer cells at 50, 100, 200, 400, and 800 µM concentrations over 24 h compared with their respective control groups after 24 h. These results indicate that the presence of L^1 and L^2 coordinated with a Pt(II) center leads to activation of cytotoxic properties. As a result of the analysis, the cytotoxic activity of the Pt(II) complex is more active than L^1 and L^2. In a previous study, A. A. Yadav *et al.* [115] investigated molecular mechanisms of the biological activity of the elesclo-

Table 6. Antimicrobial activity data for the L^1 and Pt(II) complex

Name of bacteria/fungus	İnhibition % L^1 (Complex)	Antibiotic	MIC (μg/mL) L^1 (Complex)
E. coli	4.9889 (8.8757)	Ampicillin	6.25 (6.25)
S. typhimurium	9.6174 (19.6877)	Ampicillin	6.25 (6.25)
S. aureus	50.9212 (63.7653)	Ampicillin	12.5 (6.25)
L. monocytogenes	47.6417 (59.3048)	Ampicillin	12.5 (6.25)
B. cereus	10.5767 (15.3787)	Ampicillin	6.25 (6.25)
C. albicans	53.6662 (67.8547)	Amphotericin B	6.25 (6.25)

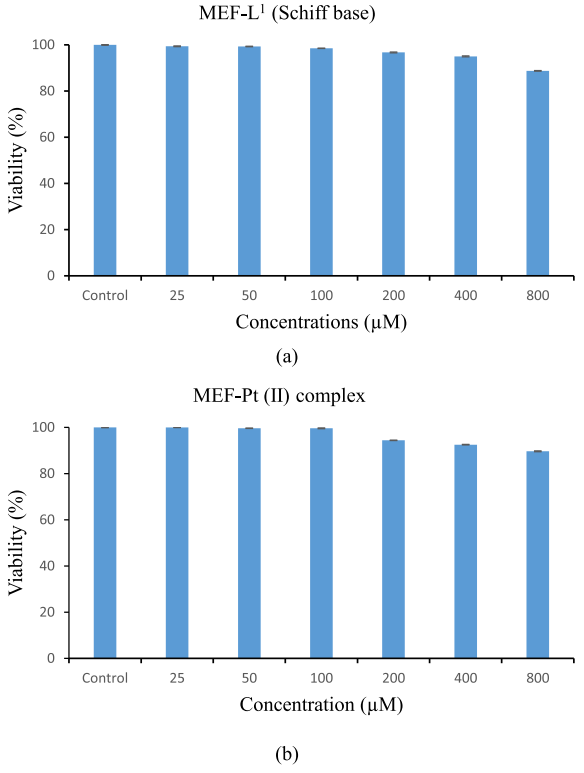

Figure 12. The viability (%) values of L^1 (a) and the Pt(II) complex (b) at different concentrations (25–800 μM) for MEF. Values are presented as the means ($n = 6$) ± S.E for 24 h.

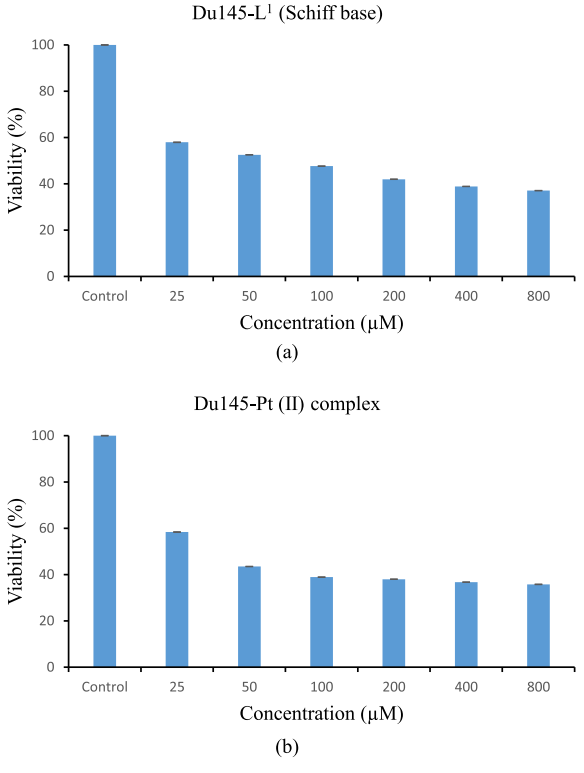

Figure 13. The viability (%) values of L^1 (a) and the Pt(II) complex (b) at different concentrations (25–800 μM) for Du145. Values are presented as the means ($n = 6$) ± S.E for 24 h.

mol and its complexes with Cu(II), Ni(II), and Pt(II). In their study, for the mechanism of biological activity of metal–elesclomol complex, they proposed that the metal(II) was selectively transported to the mitochondria and enzymatic or non-enzymatic reduction of the metal(II) deposited in the mitochondria would yield metal. They also proposed that after reduction and dissociation of the complex, the elesclomol was effluxed from the cell and continued to shuttle more metal(II) into the cell [116]. The same result may be suggested for the mechanism of the cytotoxicity activity of our Pt(II) complex.

3.6. *Antioxidant activity results*

Free radicals, which are included in the process of lipid peroxidation, are considered to play a major role in medicine. A compound with radical reducing power may serve as a potential antioxidant. Antioxidants are free radical scavengers that may prevent, protect, or reduce the extension of oxidative damage. The DPPH (2,2-diphenyl-1-picrylhydrazyl) test [117–121] is commonly used to evaluate the ability of compounds to act as free radical scavengers or hydrogen donors, and to assess antioxidant activity. The DPPH assay is performed quickly and easily with the UV–Visible spectrophotometer, which explains the widespread use in antioxidant studies. DPPH is a stable nitrogen radical, which does not resemble transient peroxyl radicals in lipid peroxidation. Many antioxidants that react quickly with peroxyl radicals may react slowly with DPPH or be ineffective on DPPH due to steric hindrance. The effect of antioxidants on DPPH radical scavenging is due to the hydrogen donating ability or radical scavenging activity of the samples [122]. A freshly prepared DPPH solution exhibits a dark purple color with maximum absorption at 517 nm because of the DPPH free radical. This purple color usually disappears when it reacts with an antioxidant that can donate electrons to the DPPH radical and DPPH converts to a stable yellow compound (DPPH–H) [102,117]. Therefore, antioxidant molecules can quench DPPH free radicals, leading to a decrease in absorbance at 517 nm. The scavenging reaction between DPPH and an antioxidant (H–D) is shown below,

$$\underset{\text{(Purple)}}{(\text{DPPH}) + (\text{H}-\text{D})} \rightarrow \underset{\text{(Yellow)}}{\text{DPPH}-\text{H} + (\text{D})}$$

Stronger antioxidants can reduce absorbance rapidly. The IC_{50} value, defined as the concentration of the sample causing the DPPH concentration to be reduced by 50%, is calculated from the linear regression of the concentration graphs of the compounds tested against the mean percentage of antioxidant activity [123,124]. The lower the IC_{50} value, the higher the antioxidant activity of the tested samples. The antioxidant activities of L^1, L^2, and the Pt(II) complex were assessed using the DPPH radical scavenging method at different concentrations. For comparison, butylated hydroxytoluene (BHT) was used as a standard. The antioxidant results of L^1, L^2 and the Pt(II) complex are presented in Figure 14 and Table 7. The IC_{50} values of L^1, L^2 and the Pt(II) complex were calculated as 3.2, 3.6, and 2.3 μM, respectively. The antioxidant activity was significantly increased as a result of the electron withdrawing effect of the Pt^{2+} ion, which facilitates hydrogen release to reduce the DPPH radical [125]. The complex also showed significant free radical scavenging when tested against DPPH. As a result, the antioxidant activity of L^1 and L^2 were determined to be enhanced on complexation with the Pt^{2+} ion. Compared to previously reported antioxidant data, the synthesized Pt(II) complex showed significant antioxidant activity. As a result, the obtained Pt complex as an antioxidant can inhibit the oxidation of lipids or other molecules by preventing the oxidative chain reactions at low concentrations. Thus, it can prevent the damage done to the body's cells by oxygen [102,126]. In addition, it can protect the human body against the damages of reactive oxygen species produced during normal cellular functions in the body and involved in the etiopathogenesis of many chronic diseases [127].

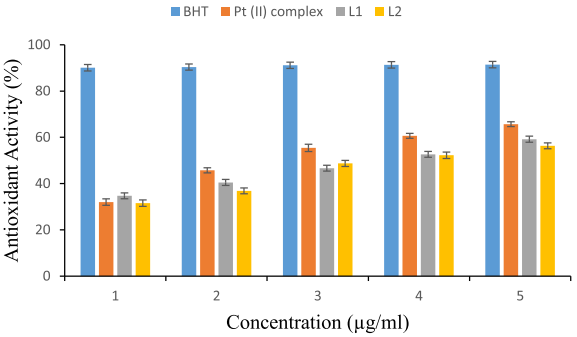

Figure 14. Percent antioxidant activity of the free ligands and Pt(II) complex ($n = 2$) ± S.E.

Table 7. IC_{50} (μM) values of antioxidant activity of the free ligands and Pt(II) complex

Compound	IC_{50} (μM)
L^1	3.2
L^2	3.6
Pt(II) complex	2.3

4. Conclusion

In this work, we studied the synthesis and spectral analysis of a Pt(II) complex of a Schiff base (L^1) derived from L-phenylalanine and furfuraldehyde in the presence 8-hydroxyquinoline (L^2). According to physico-chemical, spectrophotometric, and thermal analysis results, small shifts in spectral analysis are observed in the Pt(II) complex and the reaction of L^1 and L^2 in the presence of Pt(II) is a complex reaction. One molecule of L^1 and one molecule of L^2 react with one molecule of Pt(II) ion. The complex is active against some of the chosen bacterial and fungal strains. According to the test results, the antimicrobial activities of the complex increase compared to the antimicrobial activities of the free ligands. L^1 and the Pt(II) complex show strong cell-growth inhibition against Du145 cancer cells with MTT assay implying that they induce apoptosis in these cancer cells. Whereas L^1 is effective on Du145 cancer cells at 100, 200, 400, and 800 μM concentrations, the complex shows significant effect on Du145 cancer cells at 50, 100, 200, 400, and 800 μM concentrations over 24 h compared to the respective control groups after 24 h. The free ligands and Pt(II) complex also have significant antioxidant activity. Accordingly, the antioxidant activity results show that the complex is effective at preventing the formation of the DPPH radical. This activity is explained with chelation theory. Furthermore, the IC_{50} values observed in cytotoxicity and antioxidant activities indicate that the synthesized complex exhibits differential and selective properties.

Acknowledgments

This study was financially supported by Trakya University, Research Fund (TUBAP, project # 2016/250). We (Assoc Prof Özlen ALTUN and Research Student Melike Özge KOÇER) confirm that "Trakya University" only provided financial support within the scope of the project for chemicals in the manuscript and we declare that the support received did not lead to any conflict of interests regarding the publication of this manuscript. There is no need for Trakya University's confirmation to publish this manuscript.

Supplementary data

Supporting information for this article is available on the journal's website under article's URL https://doi.org/10.5802/crchim.9 or from the author. The experimental details and randomization protocols are provided.

References

[1] Z. Cimerman, S. Miljanic, N. Galic, *Croat. Chem. Acta*, 2000, **73**, 81-95.
[2] S. H. Rahaman, H. Chowdhury, D. Bose, R. Ghosh, C. H. Hung, B. K. Ghosh, *Polyhedron*, 2005, **24**, 1755-1763.
[3] Z. H. Chohan, M. Arif, M. Sarfraz, *Appl. Organomet. Chem.*, 2007, **21**, 294-302.
[4] Y. Li, Z. Y. Yang, T. R. Li, *Synthesis, Chem. Pharm. Bull.*, 2008, **56**, 1528-1534.
[5] İ. Şakıyan, R. Özdemir, H. Öğütçü, *Synth. React. Inorg. M.*, 2014, **44**, 417-423.
[6] A. S. Gaballa, M. S. Asker, A. S. Barakat, S. M. Teleb, *Spectrochim. Acta part A*, 2006, **67**, 114-121.
[7] S. Kumar, D. N. Dhar, P. N. Saxena, *J. Sci. Ind. Res. India*, 2009, **68**, 181-187.
[8] M. S. Suresh, V. Prakash, *J. Chem.*, 2011, **8**, 1408-1416.
[9] G. Nizami, R. Sayyed, *IOSR J. Appl. Chem.*, 2017, **10**, 40-51.
[10] M. R. Gill, J. A. Thomas, *Chem. Soc. Rev.*, 2012, **41**, 3179-3192.
[11] D. C. Carter, J. X. Ho, *Adv. Protein Chem.*, 1994, **45**, 153-203.
[12] X. M. He, D. C. Carter, *Nature*, 1992, **358**, 209-215.
[13] H. Liu, Q. Guo, J. Dong, Q. Wei, H. Zhang, X. Sun, C. Liu, L. Li, *J. Coord. Chem.*, 2015, **68**, 1040-1053.
[14] Q. Wei, J. Dong, P. Zhao, M. Li, F. Cheng, J. Kong, L. Li, *J. Photochem. Photobiol. B: Biol.*, 2016, **161**, 355-367.
[15] P. Zhao, Q. Wei, J. Dong, F. Ding, J. Li, L. Lia, *J. Coord. Chem.*, 2016, **69**, 2437-2453.
[16] H. Liu, L. Li, Q. Guo, J. Dong, J. Li, *Trans. Met. Chem.*, 2013, **38**, 441-448.
[17] Q. Guo, L. Li, J. Dong, H. Liu, T. Xu, J. Li, *Spectrochim. Acta A*, 2013, **106**, 155-162.
[18] S. Zhai, Q. Guo, J. Dong, T. Xu, L. Li, *Trans. Met. Chem.*, 2014, **39**, 271-280.
[19] D. R. Laurence, P. N. Bennett, M. J. Brown, *Antibacterial drugs, Clinical Pharmacology*, 8th ed., Churchill Livingstone, Edinburgh, Scotland, 1997, 211 pages.
[20] Z. Guo, P. J. Sadler, *Angew. Chem. Int. Ed.*, 1999, **38**, 1512-1531.
[21] O. E. Offiong, E. Nfor, A. A. Ayi, S. Martelli, *Trans. Met. Chem.*, 2000, **25**, 369-373.
[22] İ. Şakıyan, N. Gündüz, T. Gündüz, *Synth. React. Inorg. M.*, 2001, **31**, 1175-1187.
[23] İ. Şakıyan, *Trans. Met. Chem.*, 2007, **32**, 131-135.
[24] B. R. James, *Adv. Organomet. Chem.*, 1979, **17**, 319-405.
[25] F. R. Hartley, *Chem. Rev.*, 1969, **69**, 799-844.
[26] P. M. Henry, *Palladium Oxidation of Hydrocarbons Catalyzed*, D. Reidel Publishing Campany, Dordrecht, Holland, 1979, 41 pages.
[27] D. E. Webster, *Adv. Organomet. Chem.*, 1977, **15**, 147-188.

[28] C. Rimbu, R. Danac, A. Pui, *Chem. Pharm. Bull.*, 2014, **62**, 12-15.
[29] R. Mladenova, M. Ignatova, N. Manolova, T. Petrova, I. Rashkov, *Eur. Poly. J.*, 2002, **38**, 989-999.
[30] S. S. Patil, G. A. Thakur, M. M. Shaikh, *Int. Sch. Res. Network, ISRN Pharmaceutics* (2011) p. 1-6.
[31] V. Prachayasittikul, S. Prachayasittikul, S. Ruchirawat, V. Prachayasittikul, *Drug Des. Dev. Ther.*, 2013, **7**, 1157-1178.
[32] S. Srisung, T. Suksrichavalit, S. Prachayasittikul, S. Ruchirawat, V. Prachayasittikul, *Int. J. Pharm.*, 2013, **9**, 170-175.
[33] Clinical and Laboratory Standards Institute, *Reference Method for Broth Dilution Antifungal Susceptibility Testing of Yeasts: Approved Standard M27-A2*, CLSI, Wayne, PA, 2002.
[34] I. Kobayashi, H. Muraoka, T. Saika, M. Nishida, T. Fujioka, M. Nasu, *J. Med. Microbiol.*, 2004, **53**, 403-406.
[35] I. Wiegand, K. Hilpert, R. E. W. Hancock, *Nat. Protoc.*, 2008, **3**, 163-175.
[36] E. G. Kaya, H. Özbilge, S. Albayrak, *ANKEM*, 2009, **23**, 110-114.
[37] Clinical and Laboratory Standards Institute, *Performance Standards for Antimicrobial Susceptibility Testing, 15th Informational Supplement. CLSI Document M100-S22*, CLSI, PA, 2012.
[38] E. Kaya, H. Ozbilge, *Turk. J. Med. Sci.*, 2012, **42**, 325-328.
[39] M. V. Blagosklonny, A. B. Pardee, *Cancer Res.*, 2001, **61**, 4301-4305.
[40] L. Giovagnini, L. Ronconi, D. Aldinucci, D. Lorenzon, S. Sitran, D. Fregona, *J. Med. Chem.*, 2005, **48**, 1588-1595.
[41] R. Kim, M. Emi, K. Tanabe, *Cancer Chemoth. Pharm.*, 2006, **57**, 545-553.
[42] P. Z. Lu, C. Y. Lai, W. H. Chan, *Int. J. Mol. Sci.*, 2008, **9**, 698-718.
[43] S. H. Liu, C. Chen, R. S. Yang, Y. P. Yen, Y. T. Yang, C. Tsai, *J. Orthop. Res.*, 2011, **29**, 954-960.
[44] O. Doganlar, Z. B. Doganlar, *Biomed. Res.*, 2016, **27**, 268-278.
[45] T. Mossman, *J. Immunol.*, 1983, **65**, 55-63.
[46] S. Sathiyaraj, R. J. Butcher, C. Jayabalakrishnan, *J. Mol. Struct.*, 2012, **1030**, 95-103.
[47] M. S. Blois, *Nature*, 1958, **181**, 1199-1200.
[48] K. Shimada, K. Fujikawa, K. Yahara, T. Nakamura, *J. Agric. Food Chem.*, 1992, **40**, 945-948.
[49] B. Tanti, A. K. Buragohain, L. Guring, D. Kakati, A. K. Das, S. P. Borah, *Indian J. Nat. Prod. Resour.*, 2010, **1**, 17-21.
[50] A. Choudhary, R. Sharma, M. Nagar, M. Mohsin, H. S. Meena, *J. Chil. Chem. Soc.*, 2011, **56**, 911-917.
[51] O. A. El-Gammal, M. M. Mostafa, *Spectrochim. Acta Part A*, 2014, **127**, 530-542.
[52] P. Kavitha, K. L. Reddy, *Arab. J. Chem.*, 2016, **9**, 640-648.
[53] W. J. Geary, *Coord. Chem. Rev.*, 1971, **7**, 81-122.
[54] S. F. A. Kettle, *Coordination Compounds*, Thomas Nelson, London, 1975.
[55] J. R. Dyer, *Application of Absorption Spectroscopy of Organic Compounds*, Prentice-Hall, New Jersey, 1965.
[56] O. Siimann, J. Fresco, *J. Am. Chem. Soc.*, 1970, **92**, 2652-2656.
[57] A. B. P. Lever, *Inorganic Electronic Spectroscopy*, Elsevier, New York, 1984.
[58] R. K. Agarwal, S. Prasad, *Turk. J. Chem.*, 2005, **29**, 289-298.
[59] S. S. Ezzat, *Rafidain J. Sci.*, 2008, **19**, 42-47.
[60] J. G. Kang, D. H. Cho, C. Park, S. K. Kang, I. T. Kim, S. W. Lee, H. H. Lee, Y. N. Lee, D. W. Lim, S. J. Lee, S. H. Kim, Y. J. Bae, *Bull. Korean Chem. Soc.*, 2008, **29**, 599-603.
[61] S. M. S. Jambi, S. S. Kandil, *J. Mater. Environ. Sci.*, 2012, **3**, 591-604.
[62] K. Nakamato, V. Morimoto, A. E. Martelli, *J. Am. Chem. Soc.*, 1961, **83**, 4528-4532.
[63] J. B. Lambert, H. F. Shurwell, L. Verbit, R. G. Cooks, G. H. Stout, *Organic Structural Analysis*, Mac Millan, New York, 1976.
[64] G. Socrates, *Infrared Characterization Group Frequencies*, John Wiley, New York, 1980.
[65] K. Nakamato, *Infrared and Raman Spectra of Inorganic and Coordination Compounds*, 4th ed., John Wiley and Sons, New York, 1986.
[66] M. S. İslam, M. S. Ahmed, S. C. Pal, Y. Reza, S. Jesmin, *Indian J. Chem.*, 1995, **34 A**, 816-818.
[67] K. Nakamato, *Infrared and Raman Spectra of Inorganic and Coordination Compounds*, 5th ed., John Wiley, New York, 1997.
[68] I. T. Ahmed, A. A. A. Boraei, *J. Chem. Eng. Data*, 1998, **43**, 459-464.
[69] M. A. El-Gahami, Z. A. Khafagy, A. M. M. Ali, N. M. İsmail, J. Inorg, *Organomet. Polym.*, 2004, **14**, 117-129.
[70] S. Katayama, Y. Akahori, H. Mori, *Chem. Pharm. Bull.*, 1973, **21**, 2622-2626.
[71] A. A. Fomichev, Y. S. Ryabokobylko, A. V. Kessenikh, A. Ataev, B. V. Parusnikov, I. A. Krasavin, V. M. Dziomko, *Chem. Heterocycl. Com.*, 1977, **13**, 996-997.
[72] L. Jin, İ. Sakıyan, N. S. Gonzales, D. Lane, S. Cherala, *Inorg. Chim. Acta Part A*, 2014, **423**, 72-78.
[73] P. G. Jones, *Chemistry in Britain*, 1981, **17**, 222-225.
[74] P. Van Der Sluis, A. M. F. Hezemans, J. Kroon, *J. Appl. Crystallogr.*, 1989, **22**, 340-344.
[75] M. Zhang, Y. Li, Z. Yan, J. Jing, J. Xie, M. Chen, *Electrochim. Acta*, 2015, **158**, 81-88.
[76] C. S. Dilip, V. Thangaraj, A. P. Raj, *Arab. J. Chem.*, 2016, **9**, S731-S742.
[77] M. D. Udayagiri, N. G. Yernale, B. H. M. Mruthyunjayaswamy, *Int. J. Pharm. Pharm. Sci.*, 2016, **8**, 344-351.
[78] M. A. Salem, E. A. Bakr, H. G. El-Attar, *Spectrochim. Acta Part A*, 2018, **188**, 155-163.
[79] B. E. Warren, *X-ray Diffraction*, 2nd ed., Dover, New York, 1990.
[80] D. Arish, M. S. Nair, *Arab. J. Chem.*, 2012, **5**, 179-186.
[81] A. H. Atta, A. I. El-Shenawy, M. S. Refat, K. M. Elsabawy, *J. Mol. Struct.*, 2013, **1039**, 51-60.
[82] S. P. Velammal, T. A. Devi1, T. P. Amaladhas, *J. Nanostruct. Chem.*, 2016, **6**, 247-260.
[83] F. A. Al-Saif, *Int. J. Electrochem. Sci.*, 2014, **9**, 398-417.
[84] M. V. Lokhande, *Int. J. Curr. Res. Chem. Pharm. Sci.*, 2015, **2**, 89-98.
[85] H. F. G. Barbosa, M. Attjioui, A. P. G. Ferreira, E. R. Dockal, N. E. El Gueddari, B. M. Moerschbacher, E. T. G. Cavalheiro, *Molecules*, 2017, **22**, 1-19.
[86] H. B. Pedersen, J. Josephsen, G. Kerszman, *Chem. Biol. Interact.*, 1985, **54**, 1-8.
[87] S. Carotti, A. Guerri, T. Mazzei, L. Messori, E. Mini, P. Orioli, *Inorg. Chim. Acta*, 1998, **281**, 90-94.

[88] F. Abbate, P. Orioli, B. Bruni, G. Marcon, L. Messori, *Inorg. Chim. Acta*, 2000, **311**, 1-5.
[89] A. Casini, M. C. Diawara, R. Scopelliti, S. M. Zakeeruddin, M. Gratzel, P. J. Dyson, *Dalton Trans.*, 2010, **39**, 2239-2245.
[90] V. Amani, A. Abedi, S. Ghabeshi, H. R. Khavasi, S. M. Hosseini, N. Safari, *Polyhedron*, 2014, **79**, 104-115.
[91] H. C. Chen, D. G. H. Hetterscheid, R. M. Williams, J. I. Van Der Vlugt, J. N. H. Reek, A. M. Brouwer, *Energy Environ. Sci.*, 2015, **8**, 975-982.
[92] O. Altun, H. Akbaş, E. Dolen, *Spectrochim. Acta Part A*, 2007, **66**, 499-502.
[93] O. Altun, S. Bilcen, *Spectrochim. Acta Part A*, 2010, **75**, 789-793.
[94] O. Altun, M. Suozer, *J. Mol. Struct.*, 2017, **1149**, 307-314.
[95] A. S. Meyer, G. H. Ayres, *J. Am. Chem. Soc.*, 1957, **79**, 49-53.
[96] P. Job, *Ann. Chim.*, 1928, **9**, 113-203.
[97] P. Job, *Ann. Chim.*, 1936, **6**, 97-105.
[98] N. R. Filipovic, I. Markovic, D. Mitic, N. Polovic, M. Milcic, M. Dulovic, M. Jovanovic, M. Savic, M. Niksic, K. Andelkovic, T. Todorovic, *J. Biochem. Mol. Toxicol.*, 2014, **28**, 99-110.
[99] A. A. S. Al-Hamdani, A. M. Balkhı, A. Falah, S. A. Shaker, *J. Chil. Chem. Soc.*, 2015, **60**, 2774-2785.
[100] E. Pahontu, C. Paraschivescu, D. C. Ilies, D. Poirier, C. Oprean, V. Paunescu, A. Gulea, T. Rosu, O. Bratu, *Molecules*, 2016, **21**, 674-1-18.
[101] R. S. Joseyphus, M. S. Nair, *Mycobiology*, 2008, **36**, 93-98.
[102] I. P. Ejidike, P. A. Ajibade, *Molecules*, 2015, **20**, 9788-9802.
[103] T. D. Thangadurai, K. Natarajan, *Trans. Met. Chem.*, 2001, **26**, 500-504.
[104] M. A. Neelakantan, S. S. Marriappan, J. Dharmaraja, T. Jeyakumar, K. Muthukumaran, *Spectrochim. Acta A*, 2008, **71**, 628-635.
[105] N. Farrell, *Coord. Chem. Rev.*, 2007, **252**, 1-31.
[106] W. Hernandez, J. Paz, A. Vaisberg, E. Spodine, R. Richter, L. Beyer, *Bioinorg. Chem. Appl.*, 2008, **10**, 1-9.
[107] A. Bakalova, R. Buyukliev, G. Momekov, D. Ivanov, *J. Chem. Technol. Metall.*, 2013, **48**, 631-636.
[108] L. J. Li, C. Wang, C. Tian, X. Y. Yangi, X. X. Hua, J. L. Du, *Res. Chem. Intermediat.*, 2013, **39**, 733-746.
[109] V. Volarevic, J. M. Vujic, M. Milovanovic, T. Kanjevac, A. Volarevic, S. R. Trifunovic, N. Arsenijevic, *J. BUON*, 2013, **18**, 131-137.
[110] J. Pranczk, D. Jacewicz, D. Wyrzykowski, L. Chmurzynski, *Curr. Pharm. Anal.*, 2014, **10**, 2-9.
[111] K. A. Abu-Safieh, A. S. Abu-Surrah, H. D. Tabba, H. A. Al-Masri, R. M. Bawadi, F. M. Boudjelal, L. H. Tahtamouni, *J. Chem.*, 2016, 1-7.
[112] V. Simic, S. Kolarevic, I. Brceski, D. Jeremic, B. Vukovic-Gacic, *Turk. J. Biol.*, 2016, **40**, 661-669.
[113] A. Y. Shen, S. N. Wu, C. T. Chiu, *J. Pharm. Pharmacol.*, 1999, **51**, 543-548.
[114] A. Y. Shen, C. P. Chen, S. Rofffler, *Life Sci.*, 1999, **64**, 813-825.
[115] A. A. Yadav, D. Patel, X. Wu, B. B. Hasinoff, *J. Inorg. Biochem.*, 2013, **126**, 1-6.
[116] M. Nagai, N. H. Vo, L. S. Ogawa, D. Chimmanamada, T. Inoue, J. Chu, B. C. Beaudette-Zlatanova, R. Lu, R. K. Blackman, J. Barsoum, K. Koya, Y. Wada, *Free Radic. Biol. Med.*, 2012, **52**, 2142-2150.
[117] H. N. Elena, C. T. Miron, P. Gabriela, H. Mihaela, C. Titus, B. T. Alexandru, *Int. J. Mol. Sci.*, 2006, **7**, 130-143.
[118] S. Medhe, P. Bansal, M. M. Srivastava, *Appl. Nanosci.*, 2014, **4**, 153-161.
[119] V. Sanna, N. Pala, G. Dessì, P. Manconi, A. Mariani, S. Dedola, M. Rassu, C. Crosio, C. Iaccarino, M. Sechi, *Int. J. Nanomed.*, 2014, **9**, 4935-4951.
[120] K. Saritha, U. Saraswathi, *World J. Pharm. Sci.*, 2014, **2**, 1545-1551.
[121] I. P. Ejidike, P. A. Ajibade, *Bioinorg. Chem. Appl.*, 2015, 1-9.
[122] P. Arulpriya, P. Lalitha, S. Hemalatha, *Merr. Der Chem. Sin.*, 2010, **1**, 73-79.
[123] V. Saritha, R. K. Anilakumar, F. Khanum, *Int. J. Pharm. Biol. Arch.*, 2010, **1**, 376-384.
[124] N. Neelofar, N. Ali, A. Khan, S. Amir, N. A. Khan, M. Bilal, *Bull. Chem. Soc. Ethiopia*, 2017, **31**, 445-456.
[125] S. Tetteh, D. K. Dodoo, R. Appiah-Opong, I. Tuffour, *J. Inorg. Chem.*, 2014, 1-7.
[126] S. Tachakittirungrod, S. Okonogi, S. Chowwanapoon-pohn, *Food Chem.*, 2007, **103**, 381-388.
[127] D. L. Madhavi, S. S. Deshpande, D. K. Salunkhe, *Food Antioxidants: Technological, Toxicological, Health Perspective*, Marcel Dekker, New York, 1996.